

Curriculum Learning and Imitation Learning for Model-free Control on Financial Time-series

Woosung Koh^{1*}, Insu Choi^{2*}, Yuntae Jang^{1*}, Gimin Kang², Woo Chang Kim²

¹ Yonsei University

² Korea Advanced Institute of Science and Technology

{reiss.koh, jytfdsa1218}@yonsei.ac.kr, {jl.cheivly, kgm4752, wkim}@kaist.ac.kr

Abstract

Curriculum learning and imitation learning have been leveraged extensively in the robotics domain. However, minimal research has been done on leveraging these ideas on control tasks over highly stochastic time-series data. Here, we theoretically and empirically explore these approaches in a representative control task over complex time-series data. We implement the fundamental ideas of curriculum learning via data augmentation, while imitation learning is implemented via policy distillation from an oracle. Our findings reveal that curriculum learning should be considered a novel direction in improving control-task performance over complex time-series. Our ample random-seed out-sample empirics and ablation studies are highly encouraging for curriculum learning for time-series control. These findings are especially encouraging as we tune all overlapping hyperparameters on the baseline—giving an advantage to the baseline. On the other hand, we find that imitation learning should be used with caution.

Introduction

By the end of 2020, the total assets under management reached \$100 trillion U.S. dollar mark (Heredia et al. 2021). Optimizing investment portfolios and trading the markets has been an ongoing challenge, especially as literature has criticized human managers’ discretionary management of funds (Fama 1995). With the immense capital at risk and heightened competition for management fees, optimizing investment decisions continues to be an active area of research for the machine learning and control discipline (Gupta et al. 2019; Ma, Han, and Wang 2021; Pinelis and Ruppert 2022).

Despite the interest, a fundamental challenge plagues the financial control domain—fixed access to the data-generating process p_{data} . Concretely, the training data \hat{p}_{data} , which is a sampled approximation to p_{data} , is fixed and can not be further sampled without the passage of time.

We draw parallels to the robotics domain. The p_{data} in physical systems encompass the manipulator and the manipulated object(s). The sample size of \hat{p}_{data} can be raised arbitrarily via real simulations (Kalashnikov et al. 2018, 2021),

or physics simulators running in parallel (Austin et al. 2020; Makoviychuk et al. 2021).

This is unavailable to the financial control domain as we must work with a unique set of input and output features of interest, and its mapping distribution we approximate can only be sampled over the temporal dimension. Each joint stochastic processes of financial variables are distributed uniquely. \hat{p}_{data} of interest can not be reasonably proxied by other variables where more samples of \hat{p}_{data} may exist.

This results in a domain-specific need for improved signal learning and optimization with limited noisy data. Here, we explore two highly leveraged approaches in the physical control domain: (i) Curriculum Learning (CL) and (ii) Imitation Learning (IL) to best use the fixed samples of \hat{p}_{data} . Despite the integral nature of CL and IL in the physical control domain (Kilinc and Montana 2021; Berg, Caggiano, and Kumar 2023; Haldar et al. 2023; Reuss et al. 2023), it has been rarely explored for control over financial time-series.

To leverage these paradigms, we work with model-free Reinforcement Learning (RL) (Degrís, Pilarski, and Sutton 2012)—ensuring that our approach universally applies to all financial control tasks. By bridging the gap between the ample IL and CL approaches in the physical control domain and the financial control domain, we discover noteworthy improvements in generalized performance.

Through the theoretical and empirical study, our contributions are as follows:

- To the best of our knowledge, the first curriculum learning approach for financial control
- Extensive out-sample empirical results that beat up-to-date baselines for all three underlying algorithms
- Demonstrated on two representative data sets simulating inter-asset-class and intra-asset-class problems, with each optimization problem constrained differently to simulate real-world problems
- The statistical significance of our approach is especially notable as the overlapping hyperparameters are tuned for the baseline—giving an advantage to the baselines
- Analysis of curriculum learning and imitation learning approaches under a unified statistical framework of signal and noise decomposition

*These authors contributed equally.

Related Works

Curriculum Learning

Curriculum Learning (CL) has been a powerful tool in training deep learning and RL systems. Inspired by teaching a human student, the data set is augmented s.t. the network is first exposed to easier data and sequentially exposed to more challenging data (Wang, Chen, and Zhu 2021). This framework has been applied to training non-sequential tasks, such as computer vision classification (Hacohen and Weinshall 2019), and more commonly used on sequential tasks that leverage RL (Portelas et al. 2021; Narvekar et al. 2020). Recently, a work has leveraged CL in forecasting financial revenue (Koenecke and Gajewar 2020). To the best of our knowledge, no literature explores the potential for CL in high noise-to-signal complex financial systems—i.e., the financial market. Specifically, it does not leverage CL in an end-to-end control-task problem.

Imitation Learning

Imitation Learning (IL), synonymous with Learning from Demonstrations (LfD) and Behaviour Cloning (BC), is a critical approach in the robotics control learning domain (Hsiung et al. 2022). In short, IL and its variants aim to converge to an optima for the *student* (an agent we want to train) via imitating the behavior of a *teacher*, also called *expert*, or *oracle* (Hsiung et al. 2022). The extensive literature on IL in autonomous physical control highlights the strengths of IL (Ravichandar et al. 2020). Concretely, IL is highly useful when there is no tractable label generator with enough fidelity for training. IF is also highly sample efficient as it allows the student to quickly converge its learned parameters to a near-optimal region in the high-dimensional parameter space. Unlike CL, more literature on leveraging IL does exist in financial control. Representative papers include (Liu et al. 2020) and (Fang et al. 2021). Liu et al.’s work imitates two experts: (i) a heuristic expert and (ii) an oracle expert with access to future data. On the other hand, the work of Fang et al. only imitates an oracle. However, as mentioned in (Goluz̃a et al. 2023), there lacks depth in exploring IL as a feasible approach for financial control.

RL for Financial Control

RL has made significant strides in financial control since 2020, leveraging large data sets and neural-networks to improve financial decision-making without relying on model assumptions. (Hambly, Xu, and Yang 2023) outlines RL’s applications in various financial tasks and its integration with deep learning techniques, highlighting the method’s growing relevance in navigating the complexities of financial markets. (Charpentier, Elie, and Remlinger 2021) presents up-to-date overview of RL techniques with applications in economics and finance. They illustrate how RL, combined with computational advances in deep learning, can address complex behavioral problems in these fields.

Preliminary: Signal and Noise

All sequential control tasks vis-à-vis interacting with public financial markets suffer from high stochasticity and the ac-

companying high noise-to-signal ratio. This can be caused by (i) innate stochasticity in the system being modeled, (ii) incomplete observability, and (iii) incomplete modeling. Modeling the financial market suffers from all three fundamental drivers. Notably, it is evident that incomplete observability and modeling are major causes. Financial markets absorb external shocks, i.e., real-world events, via information flow across time and variables. Therefore, perfectly modeling this data-generating process p_{data} requires a world model. Additionally, we can not include every financial variable in our model due to the intractably high-dimensional feature count. Even if this was feasible, there is little guarantee that it would be helpful for our model—which is very likely modeling a finite set of variables of interest. This signal and noise theory fundamentally drives our entire approach.

Denote a movement in a tradable security sec , $\Delta sec_t = sec_t - sec_{t-1} \approx \ln(sec_t/sec_{t-1})$. Here we work with a discrete time space denoted $t \in \mathcal{T} := \{1, \dots, |\mathcal{T}|\}$. Theoretically, we can decompose this movement into signal and noise, $\Delta sec = \Delta signal + \Delta noise$. Here, the signal is defined as the movement in sec that can be reliably approximated via mapping the given set of signals within our feature space (which is naturally observable) to future movements less $\Delta noise$. That is, given a noise-free state $\mathcal{S}_{T'}^{nf} := \{\mathbf{SIG}_{t-1}, \dots, \mathbf{SIG}_{t-T'}\}$, where $T' \in \mathbb{N}$, $\mathbf{SIG}_t := \{\Delta signal_t^1, \dots, \Delta signal_t^M\}$, $m \in \mathbb{N}$, $\exists \mathcal{F}$ s.t. $\mathcal{F} : \mathcal{S}_{T'}^{nf} \mapsto \{\Delta signal_t^1, \dots, \Delta signal_t^M\}$, where an expressive \mathcal{F} approximator, $\hat{\mathcal{F}}$ performs reasonably well. Naturally, $\Delta noise_t$ is i.i.d. distributionally symmetrical system noise. The theoretical existence of a reasonable mapping function is salient as it allows us to theoretically decompose market movements $\Delta \mathcal{M} := \bigcup_{sec \in \mathcal{M}} \{\Delta sec\}$ into movements that influence future time steps, influenced by previous time steps, and the remaining movements that are noise.

Fundamentally, as noise-to-signal $\triangleq \Delta noise/\Delta signal$ rises, it is more challenging to train gradient-based learning models—i.e., sample efficiency and accuracy fall while variance rises. The challenge with modeling stochastic time series data is that \exists noise in the input ($t - n$) and label (t) space. Eliminating the noise is challenging as signal and noise decomposition can only be approximated as a posteriori. That is, accurately decomposing ($t - n$) data before (t) is available is not possible as we can not evaluate $\hat{\mathcal{F}}$. Our methods examine possible ways of reducing the $\Delta noise$ in training the control model while minimally impacting the $\Delta signal$.

Method

Portfolio Control as a Markov Decision Process

A granular range of sequential financial control tasks exists. These tasks fall under the umbrella of trading, portfolio optimization, optimal execution, or a combination of these. All these tasks interact with the market via increasing, decreasing, or maintaining a position on a discrete universe set, $\mathcal{U} := \{sec_1, \dots, sec_n, \dots, sec_N\}$ where $n \in \mathbb{N}$, via a discrete action set, $\mathcal{A} := \{a_1, \dots, a_M \mid a_m \in \{1 :$

long, 0 : none, -1 : short}, $m \in \mathbb{N}$ and discrete quantity set, $\mathcal{Q} := \{q_1, \dots, q_N \mid q \geq 0\}$. Let $\mathcal{P} := \{price_1, \dots, price_N \mid price_n \text{ corresponds to } sec_n \in \mathcal{U}\}$. When sets \mathcal{Q} , \mathcal{A} , and \mathcal{P} are expressed as matrices with appropriate dimension space, $\forall t \in \mathcal{T} \setminus |\mathcal{T}|, \exists$ transition model $\mathbb{T} : \mathcal{Q}^T \mathcal{A}^T \mathcal{P} \mapsto \mathcal{S}_{t+1}$. In the case of portfolio optimization, it is assumed that the portfolio size and in turn, the trading volume is sufficiently large relative to $p_n \in \mathcal{P}$ s.t. the optimization problem can be represented via continuous action space, simplifying the problem into $\mathbb{T} : \mathcal{W}^T \mathcal{P} \mapsto \mathcal{S}_{t+1}$, where typically the weight set, $\mathcal{W} = \{w_1, \dots, w_N \mid \sum_N w_n = 1\}$. Deviations in \mathcal{W} depend on the availability of shorting and acceptable financial leverage defined by the modeler. Concretely, for a sufficiently large volume, $|\mathcal{Q}^T \mathcal{A}| \gg 0$, such as $|\mathcal{Q}^T \mathcal{A}| \rightarrow \infty$, the discrete interaction with the market can be closely approximated via a continuous interaction model. A key advantage to modeling trading with weights is the ease of incorporating portfolio constraints. It is often the case that a modeler’s capital is finite and limited. Integrating these limits is convenient in weight-based optimization as it is implicitly modeled. We take advantage of this approach.

Ideally, the Markov Decision Process (MDP)’s state, \mathcal{S}^{MDP} , includes all relevant variables that contribute as a signal for optimal policy, π^* . However, with the virtually infinite variable combinations that could potentially make up \mathcal{S}^{MDP} the optimal state space, \mathcal{S}^{MDP*} is intractable. Instead, discretionarily including relevant variables based on domain knowledge is common. Commonly, elements of \mathcal{S}^{MDP} include lagged information on \mathcal{U} and other relevant variables. The MDP details are as in Table 1, unless stated otherwise. The Macro ETFs environment’s \mathcal{S} includes lagged values $\mathcal{U}_{T'}$ and major macroeconomic financial variables $\mathcal{M}_{T'}$. The exact state representation fed into the neural-network is available in Appendix Section 2.

Imitation Learning for Financial Control

In a single-learner setting, we call vanilla learner—it must map $\pi_\theta^{vanilla} : \mathcal{S}_{T'} \mapsto \mathcal{A}$, s.t. $arg \max_\theta \mathbb{E}(r \in \mathcal{R} | \mathcal{S}_{T'}, \pi_\theta)$. This mapping can be decomposed into two stages: (i) temporal signal representation and learning and (ii) output vector optimization given portfolio constraints. The first stage represents the implicit learning of the future state—i.e., learning the causal signal. The second stage represents forming the output vector \mathcal{A} s.t. it optimizes conforming to the environment setting—primarily, the portfolio constraint.

E.g., in the first, upstream stage, a naïve π , π^n notices that given a certain state vector direction and magnitude, in the next time step sec_1, sec_2, sec_3 , and sec_4 rise. To a π^n this signals a long (buy) position allocation $\forall sec$ resulting in a naïve signal: $\{1, 1, 1, 1\}$ corresponding to $w(a) := 1/4, \forall a \in \mathcal{A}$, weight allocation $\forall sec$, given that a linear normalization is applied to conform to portfolio constraints. A more sophisticated π , will incorporate the second, downstream stage. Within the neural-network it will transform this signal to a vector \mathcal{A} s.t. it maximizes the reward while conforming to the constraints of the environment. Concretely, a sophisticated π will learn that too many

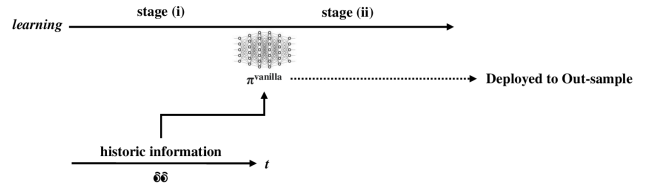


Figure 1: Training an end-to-end vanilla learner

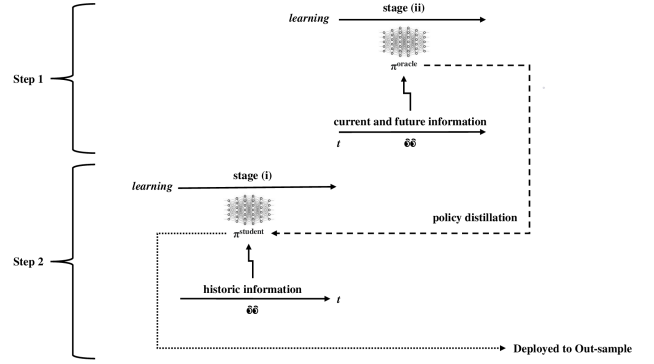


Figure 2: Training an oracle and student via IL

buy signals dilute the weight, and in turn choose to output a signal that is more concentrated for higher return probability sec s.t. $arg \max_\theta \mathbb{E}(r \in \mathcal{R} | \mathcal{S}_{T'}, \pi_\theta)$. E.g., given that the signal suggests higher confidence of sec_1 rising, it may $\mathcal{A} := \{1, 0, 0, 0\}$.

In the imitation learning paradigm, these two components are detached into two different learners. The oracle ϕ , first identifies the $\pi^\phi = \pi^*$, which conforms to environmental constraints. ϕ can trivially identify π^* as it has access to future data. The student learner incorporating $a^* \in \pi^*$ can directly learn to conform to an environment-constrained optimal policy. Simply put, the teacher strictly learns stage (ii) while the student focuses on stage (i). By delegating the two stages to two distinct learners, the student learner, in theory, can more efficiently tune its high-dimensional parameters θ . The intuition is visualized in Figures 1 and 2.

ϕ is optimized by $\pi_\theta^* := arg \min_\theta -\mathbb{E}(r \in \mathcal{R}^\phi | \mathcal{S}^\phi, \pi_\theta)$ where \mathcal{R} is the accumulated reward of the trajectory, and \mathcal{S}^ϕ is the oracle’s state set which includes *current and future data*, as previous data is irrelevant in optimizing for stage (ii). Here, $r \in \mathcal{R}^\phi$ is generated via the portfolio’s log return. The control task, $\pi^\phi : \mathcal{S}^\phi \mapsto \mathcal{A}$ mapping can be optimized with any approach. The approaches can be largely divided into dynamical programming and learning-based approaches. Here we choose a learning-based MDP approach, namely actor-critic RL algorithms, Trust Region Policy Optimization (TRPO) (Schulman et al. 2015), Proximal Policy Optimization (PPO) (Schulman et al. 2017), and Advantage Actor-Critic (A2C) (Mnih et al. 2016). These actor-critic approaches utilize both a policy (actor) and value (critic) network, which optimizes the state-action pair and state-value pair respectively, and finally combines the two into a sin-

Table 1: Markov decision process

Environment	Macro ETFs	Commodity Futures
Universe, \mathcal{U}	$\{ETF_1, \dots, ETF_4\}$	$\{F_1, \dots, F_8\}$
State, \mathcal{S}	$\{\mathcal{U}_{T'}, \mathcal{M}_{T'}\}$	$\{\mathcal{U}_{T'}\}$
Action, \mathcal{A}	$\{a_1, \dots, a_4 \mid a \in \{-1, 0, 1\}\}$	$\{a_1, \dots, a_8 \mid a \in \{-1, 0, 1\}\}$
Reward, $r \in \mathcal{R}$	$\ln(portfolio_t/portfolio_{t-1})$	$\ln(portfolio_t/portfolio_{t-1})$

gle actor-critic algorithm. Neural-network-based MDP approaches are ideal for our problem as we attempt to identify a framework that can be applied universally across all financial sequential control tasks.

Due to \mathcal{S}^ϕ , the optimal action at each time step $\pi^*(\mathcal{S}_t)$ is easily extractable. Policy optimization at each time step is trivial as ϕ has access to future values. Next, we distill the optimal policy via IL. Student ψ is optimized by $\pi_\theta^\psi = \arg \min_\theta -\mathbb{E}(r \in \mathcal{R}^\psi | \mathcal{S}^\psi, \pi_\theta)$, where $\mathcal{S}^\psi \equiv \mathcal{S}_{T'}$. The policy function $\pi^\psi : \mathcal{S}^\psi \mapsto \mathcal{A}$ is far more challenging as \mathcal{S}^ψ only has access to lagged data. I.e., it is responsible for stage (i) mentioned at the beginning of this section. Here, instead of setting the $r \in \mathcal{R}$ to the portfolio’s log return, $r \in \mathcal{R}^\psi := -distance(\mathcal{A}^\psi, \mathcal{A}^\phi = \mathcal{A}^*)$, in turn allowing π^ψ to learn via the π^ϕ which theoretically reduces $\Delta noise$ in the label space. We set $distance(\cdot, \cdot)$ to the $\|\delta\|_2$ distance of the two vectors. As the learning algorithm aims to maximize the similarity of the two policy vectors—it equivalently aims to minimize the distance. Since π^ϕ and subsequently \mathcal{A}^ϕ is retrieved from offline data, \mathcal{A}^ϕ is only known as a posteriori—making it deterministic. The $\|\delta\|_2$ too is a deterministic mapping. Concretely, it would only be possible to retrieve a reliable stochastic π^ϕ if we could simulate parallel worlds—which we know is intractable.

(Fang et al. 2021)’s IL algorithm is named Oracle Policy Distillation (OPD), and it is trained via a linear combination of the return (the vanilla learner’s reward) and the dissimilarity with the oracle. Our IL algorithm only uses the dissimilarity with the oracle, to examine a direct, pure form of IL. We hereforth refer to it as Direct Policy Distillation (DPD). The pseudo-code for the training process of IL approaches are available in Appendix Section 5.

Curriculum Learning for Financial Control

Our application of the CL paradigm takes an alternative approach in dealing with the $\Delta noise$. In the IL paradigm, the labels provided to the student is theoretically $\Delta noise$ -free, however, this comes with removing a lot of the $\Delta signal$ in the label. This is consistent with our previous discussions mentioning that the per time step $\Delta signal$, and $\Delta noise$ is only decomposable as a posteriori and is, for practical purposes—intractable.

We implement the CL paradigm by smoothening the noisy time-series data during training. We hypothesize that minor data smoothing will reduce $\Delta noise$ more than $\Delta signal$, improving signal learning and out-sample performance. We attempt two types of data smoothing: (i) exponential moving averages (EMA) and (ii) rounding. Rounding is implemented as:

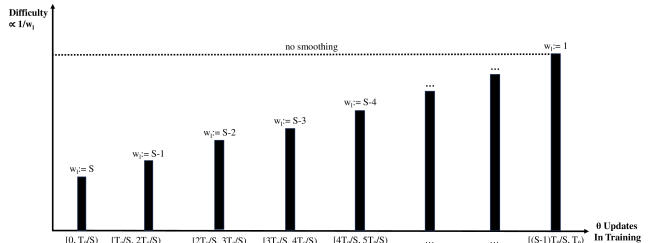


Figure 3: Inverse smoothing

$$\Delta sec_t^{rounded} \leftarrow round(\Delta sec_t, 2) \quad (1)$$

where the second parameter represents the decimal places.

We prioritize EMA-based approaches because rounding is arbitrary, with less theoretical foundation than EMA. Our implementation of the EMA is defined recursively:

$$\Delta sec_t^{EMA} \leftarrow \alpha \cdot \Delta sec_t + (1 - \alpha) \cdot \Delta sec_{t-1}^{EMA} \quad (2)$$

$$\alpha := 2/(w_l + 1) \quad (3)$$

where w_l is the lagging window hyperparameter. \forall EMA-based implementation, we concatenate w_l to the end of the method name string.

The first approach we test is EMA5, where the training is done on EMA5 smoothed data. The second approach we test is Inverse-Smoothing (IS), directly inspired by CL. Given S , we let $w_l \leftarrow S$ and train the network in w_l distinct stages, with the first stage being the most smoothened, while the subsequent stage is $w_l \leftarrow w_l - 1$. This results in the final stage having no smoothing as $w_l \leftarrow 1$. Each stage is assigned an equal number of θ updates, as shown in Figure 3. The pseudo-code for the training process is available in Appendix Section 7.

Data

We select two representative data sets in the financial time series domain to test our ideas. The financial variables are chosen based on the greatest trading volume—i.e., how actively it is traded, which is a robust gauge of its significance in the public financial markets. Notably, two data sets are used to examine (i) inter-asset-class and (ii) intra-asset-class effectiveness. That is, the first data set corresponds to a portfolio of different investment categories and financial variables, while the second data set corresponds to securities

within a single investment category. We herewith refer to Data Sets 1 and 2 as representing the Macro ETFs and Commodity Futures environments in Table 1, respectively. We visualize the stochastic time-series of \mathcal{U} in Appendix Figures 6 and 7, with black vertical lines representing the train, validation, and test split. Further details on data sourcing and processing are provided in Appendix Section 1.

Optimization Constraints

To raise the robustness of our study, we apply two hard constraints, one for each data set—mimicking real-world portfolio optimization problems. Constraint 1 (Data Set 1): The portfolio’s maximum aggregate gross exposure is 1. Equivalently, the net exposure is bound by $[-1, 1]$. Constraint 2 (Data Set 2): The portfolio’s maximum aggregate gross exposure is 2. Equivalently, the net exposure is bound by $[-2, 2]$. We use simple linear normalization to respect the hard constraints. However, softmax can also be used.

$$\begin{aligned} \theta_{ML} &= \arg \min_{\theta} -\mathbb{E}_{(\mathcal{S}_t, r \in \mathcal{R}) \sim p_{data}} \log p_{model}(r | \mathcal{S}_t; \theta) \\ &\approx \hat{\theta}_{ML} = \arg \min_{\theta} -\mathbb{E}_{(\mathcal{S}_t, r \in \mathcal{R}) \sim \hat{p}_{data}} \log p_{model}(r | \mathcal{S}_t; \theta) \end{aligned} \quad (4)$$

$$\text{subject to } -1 \leq \sum_{a \in \mathcal{A}_{\hat{g}}} w(a, \mathcal{A}_{\hat{g}}) \leq 1 \quad \forall t, \text{ for Data Set 1,}$$

$$\text{subject to } -2 \leq \sum_{a \in \mathcal{A}_{\hat{g}}} w(a, \mathcal{A}_{\hat{g}}) \leq 2 \quad \forall t, \text{ for Data Set 2.}$$

Empirical Study

By the Markov property, a non-sequential neural-network can be applied to the agent. However, to test the efficacy of a temporal encoder-decoder neural-network for the MDP environment, we examined some preliminary experiments with an LSTM architecture (Hochreiter and Schmidhuber 1997). However, we found no improvement in performance but significantly slower training and inference run-times. Therefore, our experiments are Multilayer Perceptron (MLP)-based.

First, we compare our proposed approaches’ performance against a heuristic and an RL baseline— rebalanced portfolio (RP), and no IL and CL, respectively. RP is a common approach in financial control as this heuristic has been shown to beat most professional investment managers (Cover 1991; Ye et al. 2020). Additionally, OPD is a state-of-the-art baseline for IL-based control (Fang et al. 2021). We constrain the OPD experiments to PPO as PPO is the only underlying algorithm tested by the authors of OPD. Additionally, we found it challenging to train OPD vis-à-vis run-time. That is, due to the higher computational complexity, we empirically observe and theoretically verify that the order of computational complexity is in descending order: MLP with OPD > LSTM with all else > MLP with all else. The remaining methods: {DPD, DPD-LGN, R, EMA5, IS8, TIS} are ours,

Table 2: Test Set Cumulative Return ($\pm 1\sigma$): TRPO

Method	Data Set 1	Data Set 2
Heuristic		
RP	2.951	91.057
Baseline		
TRPO	29.4402 \pm 51.712	-12.820 \pm 38.931
Imitation Learning*		
TRPO-DPD	-1.762 \pm 19.492	-0.9014 \pm 3.239
TRPO-DPD-LGN [†]	-0.187 \pm 17.948	1.849 \pm 72.434
Curriculum Learning*		
TRPO-R [‡]	21.949 \pm 61.999	-4.260 \pm 49.437
TRPO-EMA5	104.599 \pm 44.225	13.941 \pm 67.672
TRPO-IS8	31.806 \pm 29.014	49.471 \pm 112.507
TRPO-TIS [†]	111.169 \pm 44.182	-56.721 \pm 130.088

*ours, [†]ablation study, [‡]naïve approach

where {R} is a naïve approach and {DPD-LGN, TIS} are ablation studies described in detail later in this section.

Each statistic in Tables 2, 3, and 4 is by nature highly stochastic, excluding RP, which is deterministic. \forall RL-based methods, the statistics are mean $\pm 1\sigma$, where the sample size is 50. Notably, \forall inference, the model is trained with a random-seed. That is, each sample corresponds to an independently retrained model. This assures the robustness of our experiments. In aggregate, 2500 $\leftarrow (2 \cdot 8 \cdot 50 \cdot 3) + (2 \cdot 50)$ independent experiments have been conducted—(2 data sets, 8 stochastic methods, 50 samples, and 3 underlying model-free algorithms) + OPD on (2 data sets, 50 samples). We use the conventional 0.6, 0.2, and 0.2 split ratio for train, validation, and test set, respectively.

As we wish to examine the proposed methods’ training efficiency and out-sample performance, we fix the RL step-count to 1,000,000 steps of training, where the training set size < 1,000,000. We emphasize that this is unavoidable as the data set for \hat{p}_{data} is fixed, and we are unable to further sample trajectories from p_{data} . This discussion is made in the previous sections. This leads to repetitive training of the same training set. To ensure that we are not in the overfitting regime, we conducted preliminary experiments examining the validation set performance at [100,000 : 1,000,000] steps. Further details on hyperparameter tuning in the training, validation set, and inference on the test set are detailed in Appendix Sections 3, 4, 5, 6, 7, and 8.

Ablation Study

After observing the poor performances of IL approaches, and the improved performances of CL approaches, we found it imperative to further conduct *two* additional ablation studies for a better understanding of the results.

First, synthetically removing the $\Delta noise$ in the label space, as seen in OPD and DPD, consistently resulted in poor performance. The transformation to a wholly deterministic label space in the process of policy distillation caused concern about the complete lack of $\Delta noise$. We know that deep learning models can benefit from perturbations (Liu

Table 3: Test Set Cumulative Return ($\pm 1\sigma$): PPO

Method	Data Set 1	Data Set 2
Heuristic		
RP	2.951	91.057
Baselines		
PPO	29.440 \pm 51.712	4.202 \pm 64.185
PPO-OPD	23.009 \pm 48.459	-44.461 \pm 177.441
Imitation Learning*		
PPO-DPD	3.543 \pm 29.152	-24.805 \pm 79.796
PPO-DPD-LGN [†]	-3.059 \pm 35.961	-4.687 \pm 100.238
Curriculum Learning*		
PPO-R [‡]	17.028 \pm 50.973	-13.728 \pm 69.622
PPO-EMA5	81.817 \pm 33.423	35.215 \pm 55.376
PPO-IS8	81.873 \pm 39.850	39.389 \pm 134.199
PPO-TIS [†]	28.032 \pm 53.716	24.380 \pm 120.121

*ours, [†]ablation study, [‡]naïve approach

et al. 2019; Wong and Kolter 2020), and wholly removing the noise may result in diminished generalization. Therefore, we implement Learned Gaussian Noise (LGN) on top of DPD, which tunes for the diagonal covariance matrix Σ in the training and validation set. The mean vector is set to an all-zero vector to maintain the maximum likelihood properties of our optimization. With Σ , we perturb the label space. To efficiently optimize this continuous space, we use a large-scale Bayesian optimization implementation of (Kandasamy et al. 2020). Further details are available in Appendix Section 6.

The second ablation study vis-à-vis CL tunes S , $S_{searchspace} := \{1, 2, \dots, 8\}$ in the training and validation set, instead of $S := 8$. We name this approach as Tuned Inverse-Smoothing (TIS). We study whether tuning on the validation set is transferable out-sample, and the implications on the stationarity of Δ_{signal} and Δ_{noise} decomposition. Training for ablation studies are detailed in Appendix Sections 6 and 7.

Analysis and Discussion

Results

The results are summarized in Tables 2, 3, and 4 and visualized in Figures 4, 5, 8, 9, 10, and 11. Note that σ in the Tables are derived by the entire test set, while the σ in the Figures are per t . The heuristic RP achieves a 2.951% and 91.057% return in the test set. The visualization of the heuristic does not include $\pm\sigma$ as it is a deterministic policy. In the two environments, RL approaches display varying performance against the heuristic. This emphasizes the ongoing challenges of end-to-end neural-network-based control on highly stochastic time-series like financial markets. However, due to its deterministic nature, it is not possible to draw statistical conclusions that the heuristic will continue to perform well going forward. The heuristic is highly naïve, with no past information guiding future decision-making.

Within the RL-based approaches, the best result across

Table 4: Test Set Cumulative Return ($\pm 1\sigma$): A2C

Method	Data Set 1	Data Set 2
Heuristic		
RP	2.951	91.057
Baseline		
A2C	9.374 \pm 33.604	9.567 \pm 66.664
Imitation Learning*		
A2C-DPD	1.205 \pm 40.249	0.099 \pm 4.680
A2C-DPD-LGN [†]	9.613 \pm 41.123	1.043 \pm 15.055
Curriculum Learning*		
A2C-R [‡]	7.493 \pm 32.060	5.893 \pm 72.870
A2C-EMA5	40.550 \pm 24.504	104.17 \pm 75.074
A2C-IS8	46.018 \pm 28.972	41.937 \pm 106.385
A2C-TIS [†]	46.414 \pm 28.788	4.651 \pm 130.721

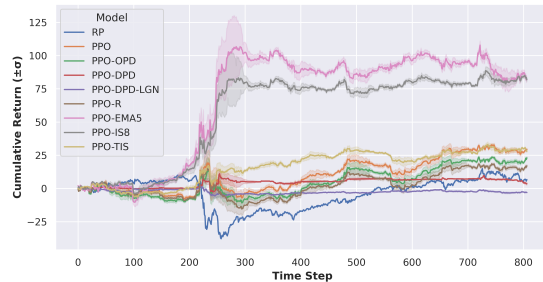
*ours, [†]ablation study, [‡]naïve approach

Figure 4: PPO Test Set Inference (Data Set 1)

the column is highlighted in bold. We observe highly encouraging signs as $\forall 6$ (2 data sets \cdot 3 underlying algorithms) empirical environments, each best result is the EMA-based CL we propose—{EMA5, IS8, TIS}. Consistent with expectations, the naïve rounding approach’s performance significantly lags the EMA-based approaches. Appendix Section 9, Tables 11, 12, and 13 presents a detailed statistical significance study.

Notably, out of the six empirical environments, EMA5 achieves statistical significance (< 0.05 P-value) all 6 times, while IS8 achieves statistical significance 5 times. The remaining non-statistically significant case still shows improvement over all baselines—with significant improvement against the heuristic. These results are highly encouraging as all overlapping hyperparameters, $h \in \mathcal{H}$ have been tuned for the baseline underlying algorithm, suggesting more room for improvement in our proposed methods on the training and validation stage.

On the other hand, we observe a dramatic worsening of performance for IL approaches. First, for the case of PPO-OPD, a state-of-the-art baseline, in this limited data environment, it distinctly performs worse than its underlying algorithm—PPO in both data sets. The DPD approach, which transforms the label space from stochastic to deterministic via policy distillation, fares no better. The added



Figure 5: PPO Test Set Inference (Data Set 2)

Gaussian noise in LGN occasionally improves performance, but no statistically meaningful observation is found.

When IL approaches in Figures 4, 5, 8, 9, 10, 11 are examined in detail, it is clear that the agent has failed to learn any meaningful signal. The most extreme case can be viewed in Figure 11 where A2C-DPD and A2C-DPD-LGN refuses to take any position at all, resulting in a nearly flat test set performance. The performances of DPD, DPD-LGN, and OPD across all test set results make it obvious that minimal pattern recognition and learning has been achieved. We now analyze the results from the perspective of Δ_{signal} and Δ_{noise} decomposition.

Theoretical Implications

We begin with our first remark, which underlies the theoretical foundation for both the performance of CL and IL under the presented environment circumstances.

Remark 1 *Given a possibly infinite or at least intractably large high dimensional underlying $p_{data}(\mathcal{A} | \mathcal{S}) \forall t$ due to the nature of determining \mathcal{S} , $\exists \Delta_{noise}$ in both input and label space which adversely impacts deep reinforcement learning—which attempts to learn $\hat{p}_{data}(\mathcal{A} | \mathcal{S}_{approximate}) \forall t$.*

This remark allows us to define the second remark, which summarizes how the CL approaches improve deep reinforcement learning approaches under such circumstances.

Remark 2 *Given Remark 1, it is possible to, on average, smooth the input and label space s.t.*

$$\frac{1}{|D_T|} \sum_{d \in D_T} \frac{\partial P_G}{-(\partial \Delta_{noise}_d)} - \frac{\partial P_G}{-(\partial \Delta_{signal}_d)} > 0 \quad (5)$$

where smoothing necessarily $\partial \Delta_{noise} \leq 0$ and $\partial \Delta_{signal} \leq 0$. D_T refers to the set of data points for training, and P_G refers to generalization performance, i.e., out-sample performance.

For reasons described in previous sections, Δ_{signal} and Δ_{noise} are intractable. Therefore, we are left with indiscriminate smoothing that often leads to $\partial \Delta_{noise} < 0 \implies \partial \Delta_{signal} < 0$, $\forall \frac{\partial P_G}{-(\partial \Delta_{noise})} > 0$. Notably, our empirical study supports in-so-far the “on average” clause, as the

entire training data, including the input and label space, is smoothed identically. Despite the overwhelming evidence supporting the direct use of CL-based smoothing approaches on noisy control tasks, hyperparameter tuning the degree of smoothing can be tricky, as we observe that it shows signs of the non-stationary property.

Remark 3 *The decomposition $\Delta_{signal} + \Delta_{noise} \leftarrow \Delta_{sec}$ is likely non-stationary. I.e., $\frac{\Delta_{signal}}{\Delta_{sec}} \sim p_s$ and $\frac{\Delta_{noise}}{\Delta_{sec}} \sim p_n$ changes over the temporal dimension.*

We observe this empirically, as TIS does not always lead to the best performance. We note that the tuning only employs 1 sample per $S \in S_{searchspace}$, making it a biased estimate of the optimal hyperparameter. This is why we mention that the non-stationary property is likely in Remark 3. The claim is not statistically significant. Despite this shortcoming, we observe significant instability in the model’s ability to generalize when employing the tuned hyperparameter given in Appendix Table 8. Notably, it identified that $S \leftarrow 1$ is optimal in two of the six cases, corresponding to no CL. However, consistent with the superior performance of smoothed training data points, its performance falls dramatically in these cases. Therefore, we leave it up to future work to investigate practical workarounds to CL’s non-stationary nature of the smoothing hyperparameter.

The poor performance of IL approaches under these circumstances can be described by Remark 4.

Remark 4 *Given Remark 1, Δ_{noise} can be synthetically removed in the label space during training via policy distillation from an oracle. However, this dramatic reduction in Δ_{noise} transforms the label space from stochastic \rightarrow deterministic, losing most of the Δ_{signal} in the process.*

The mechanism of Remark 4 is carefully detailed in Appendix Section 10, which we urge the reader to examine. We believe this theoretical analysis is helpful for future research in IL approaches when the underlying system is very high dimensional—and, in turn, stochastic.

Future Works

This work opens the door to an extensive list of possible future works. The most pressing next step is to examine the non-stationary nature of the signal, noise decomposition. The results here hint at a possibly non-stationary decomposition—meaning robust CL approaches will benefit from dynamically adapting the level of smoothing over the temporal dimension. Furthermore, only a few smoothing methods have been empirically tested here. We encourage future works to attempt other smoothing methods and analyze the theoretical reasoning behind the smoothing technique.

Additionally, future works can branch out from the specific environment presented here. First, investigating other highly stochastic temporal systems and domains that may benefit from the proposed approach will be impactful. Moreover, there is no theoretical reason why the proposed CL approaches would not transfer to other learning tasks, such as forecasting.

References

- Austin, J.; Corrales-Fatou, R.; Wyetzner, S.; and Lipson, H. 2020. Titan: A Parallel Asynchronous Library for Multi-Agent and Soft-Body Robotics using NVIDIA CUDA. In *2020 IEEE International Conference on Robotics and Automation (ICRA)*, 7754–7760.
- Berg, C. H.; Caggiano, V.; and Kumar, V. 2023. SAR: Generalization of Physiological Dexterity via Synergistic Action Representation. In *Proceedings of Robotics: Science and Systems*. Daegu, Republic of Korea.
- Charpentier, A.; Elie, R.; and Remlinger, C. 2021. Reinforcement learning in economics and finance. *Computational Economics*, 1–38.
- Cover, T. M. 1991. Universal portfolios. *Mathematical finance*, 1(1): 1–29.
- Degrís, T.; Pilarski, P. M.; and Sutton, R. S. 2012. Model-free reinforcement learning with continuous action in practice. In *2012 American Control Conference (ACC)*, 2177–2182. IEEE.
- Deng, Y.; Bao, F.; Kong, Y.; Ren, Z.; and Dai, Q. 2016. Deep direct reinforcement learning for financial signal representation and trading. *IEEE transactions on neural networks and learning systems*, 28(3): 653–664.
- Dixon, M.; Klabjan, D.; and Bang, J. H. 2015. Implementing deep neural networks for financial market prediction on the Intel Xeon Phi. In *Proceedings of the 8th workshop on high performance computational finance*, 1–6.
- Fama, E. F. 1995. Random walks in stock market prices. *Financial analysts journal*, 51(1): 75–80.
- Fang, Y.; Ren, K.; Liu, W.; Zhou, D.; Zhang, W.; Bian, J.; Yu, Y.; and Liu, T.-Y. 2021. Universal trading for order execution with oracle policy distillation. In *Proceedings of the AAAI Conference on Artificial Intelligence*, volume 35, 107–115.
- Goluža, S.; Bauman, T.; Kovačević, T.; and Kostanjčar, Z. 2023. Imitation Learning for Financial Applications. In *2023 46th MIPRO ICT and Electronics Convention (MIPRO)*, 1130–1135. IEEE.
- Gudelek, M. U.; Boluk, S. A.; and Ozbayoglu, A. M. 2017. A deep learning based stock trading model with 2-D CNN trend detection. In *2017 IEEE symposium series on computational intelligence (SSCI)*, 1–8. IEEE.
- Gupta, S.; Bandyopadhyay, G.; Biswas, S.; and Upadhyay, A. 2019. A hybrid machine learning and dynamic nonlinear framework for determination of optimum portfolio structure. In *Innovations in Computer Science and Engineering: Proceedings of the Sixth ICICSE 2018*, 437–448. Springer.
- Hacohen, G.; and Weinshall, D. 2019. On the power of curriculum learning in training deep networks. In *International conference on machine learning*, 2535–2544. PMLR.
- Haldar, S.; Pari, J.; Rai, A.; and Pinto, L. 2023. Teach a Robot to FISH: Versatile Imitation from One Minute of Demonstrations. In *Proceedings of Robotics: Science and Systems*. Daegu, Republic of Korea.
- Hambly, B.; Xu, R.; and Yang, H. 2023. Recent advances in reinforcement learning in finance. *Mathematical Finance*, 33(3): 437–503.
- Heredia, L.; Bartletta, S.; Carrubba, J.; Frankle, D.; McIntyre, C.; Palmisani, E.; Panagiotou, A.; Pardasani, N.; et al. 2021. The \$100 trillion machine.
- Hochreiter, S.; and Schmidhuber, J. 1997. Long short-term memory. *Neural computation*, 9(8): 1735–1780.
- Hsiung, E.; Rosen, E.; Chi, V. B.; and Malle, B. F. 2022. Learning reward functions from a combination of demonstration and evaluative feedback. In *2022 17th ACM/IEEE International Conference on Human-Robot Interaction (HRI)*, 807–811. IEEE.
- Kalashnikov, D.; Irpan, A.; Pastor, P.; Ibarz, J.; Herzog, A.; Jang, E.; Quillen, D.; Holly, E.; Kalakrishnan, M.; Vanhoucke, V.; et al. 2018. Scalable deep reinforcement learning for vision-based robotic manipulation. In *Conference on Robot Learning*, 651–673. PMLR.
- Kalashnikov, D.; Varley, J.; Chebotar, Y.; Swanson, B.; Jonschkowski, R.; Finn, C.; Levine, S.; and Hausman, K. 2021. Scaling up multi-task robotic reinforcement learning. In *5th Annual Conference on Robot Learning*.
- Kandasamy, K.; Vysyaraju, K. R.; Neiswanger, W.; Paria, B.; Collins, C. R.; Schneider, J.; Poczos, B.; and Xing, E. P. 2020. Tuning Hyperparameters without Grad Students: Scalable and Robust Bayesian Optimisation with Dragonfly. *Journal of Machine Learning Research*, 21(81): 1–27.
- Kilinc, O.; and Montana, G. 2021. Follow the Object: Curriculum Learning for Manipulation Tasks with Imagined Goals. In *Deep RL Workshop NeurIPS 2021*.
- Koenecke, A.; and Gajewar, A. 2020. Curriculum learning in deep neural networks for financial forecasting. In *Mining Data for Financial Applications: 4th ECML PKDD Workshop, MIDAS 2019, Würzburg, Germany, September 16, 2019, Revised Selected Papers 4*, 16–31. Springer.
- Liu, H.; Ji, R.; Li, J.; Zhang, B.; Gao, Y.; Wu, Y.; and Huang, F. 2019. Universal Adversarial Perturbation via Prior Driven Uncertainty Approximation. In *2019 IEEE/CVF International Conference on Computer Vision (ICCV)*, 2941–2949. IEEE.
- Liu, Y.; Liu, Q.; Zhao, H.; Pan, Z.; and Liu, C. 2020. Adaptive quantitative trading: An imitative deep reinforcement learning approach. In *Proceedings of the AAAI conference on artificial intelligence*, volume 34, 2128–2135.
- Ma, Y.; Han, R.; and Wang, W. 2021. Portfolio optimization with return prediction using deep learning and machine learning. *Expert Systems with Applications*, 165: 113973.
- Makoviychuk, V.; Wawrzyniak, L.; Guo, Y.; Lu, M.; Storey, K.; Macklin, M.; Hoeller, D.; Rudin, N.; Allshire, A.; Handa, A.; et al. 2021. Isaac Gym: High Performance GPU Based Physics Simulation For Robot Learning. In *Thirty-fifth Conference on Neural Information Processing Systems Datasets and Benchmarks Track (Round 2)*.
- Mnih, V.; Badia, A. P.; Mirza, M.; Graves, A.; Lillicrap, T.; Harley, T.; Silver, D.; and Kavukcuoglu, K. 2016. Asynchronous methods for deep reinforcement learning. In *In-*

ternational conference on machine learning, 1928–1937. PMLR.

Narvekar, S.; Peng, B.; Leonetti, M.; Sinapov, J.; Taylor, M. E.; and Stone, P. 2020. Curriculum learning for reinforcement learning domains: A framework and survey. *The Journal of Machine Learning Research*, 21(1): 7382–7431.

Pendharkar, P. C.; and Cusatis, P. 2018. Trading financial indices with reinforcement learning agents. *Expert Systems with Applications*, 103: 1–13.

Pinelis, M.; and Ruppert, D. 2022. Machine learning portfolio allocation. *The Journal of Finance and Data Science*, 8: 35–54.

Portelas, R.; Colas, C.; Weng, L.; Hofmann, K.; and Oudeyer, P.-Y. 2021. Automatic curriculum learning for deep RL: a short survey. In *Proceedings of the Twenty-Ninth International Conference on Artificial Intelligence*, 4819–4825.

Ravichandar, H.; Polydoros, A. S.; Chernova, S.; and Billard, A. 2020. Recent advances in robot learning from demonstration. *Annual review of control, robotics, and autonomous systems*, 3: 297–330.

Reuss, M.; Li, M.; Jia, X.; and Lioutikov, R. 2023. Goal-Conditioned Imitation Learning using Score-based Diffusion Policies. In *Proceedings of Robotics: Science and Systems*. Daegu, Republic of Korea.

Schulman, J.; Levine, S.; Abbeel, P.; Jordan, M.; and Moritz, P. 2015. Trust region policy optimization. In *International conference on machine learning*, 1889–1897. PMLR.

Schulman, J.; Wolski, F.; Dhariwal, P.; Radford, A.; and Klimov, O. 2017. Proximal policy optimization algorithms. *arXiv preprint arXiv:1707.06347*.

Sezer, O. B.; and Ozbayoglu, A. M. 2018. Algorithmic financial trading with deep convolutional neural networks: Time series to image conversion approach. *Applied Soft Computing*, 70: 525–538.

Wang, X.; Chen, Y.; and Zhu, W. 2021. A survey on curriculum learning. *IEEE Transactions on Pattern Analysis and Machine Intelligence*, 44(9): 4555–4576.

Wong, E.; and Kolter, J. Z. 2020. Learning perturbation sets for robust machine learning. In *International Conference on Learning Representations*.

Ye, Y.; Pei, H.; Wang, B.; Chen, P.-Y.; Zhu, Y.; Xiao, J.; and Li, B. 2020. Reinforcement-learning based portfolio management with augmented asset movement prediction states. In *Proceedings of the AAAI Conference on Artificial Intelligence*, volume 34, 1112–1119.

Appendix

1. Data Sourcing and Processing

We obtain both data sets from S&P Capital IQ and Bloomberg to ensure the quality and consistency of the data, and to prevent look-ahead bias. We source the Bull-Bear Spread separately from the Investor Sentiment Index of the American Association of Individual Investors (AAII).

All the data used in the empirical study is available publicly and have been extensively used as benchmarks in representative studies (Dixon, Klabjan, and Bang 2015; Deng et al. 2016; Gudelek, Boluk, and Ozbayoglu 2017; Sezer and Ozbayoglu 2018; Pendharkar and Cusatis 2018).

The financial variables composing the data sets are available in Table 5 and 6. In Data Set 1, corresponding to Table 5, $\mathcal{U}_1 = \{GLD, USO, USD, LQD\}$ and $\mathcal{M}_1 = \{3M, 2Y, 10Y, FFEOR, 10Y - 3M, 10Y - 2Y, IYR, VIX, BULL_BEAR_SPREAD\}$. The initial time step is set to the date where \exists valid data points \forall variable. The Data Set 1’s date spans: [2006-04-11, 2022-07-08] in daily units. Data Set 2’s date spans: [1990-01-021, 2023-06-26] in daily units. \mathcal{U} is visualized in Figure 6 and 7, with black vertical lines representing the train, validation, and test split.

Table 5: Data Set 1 (Inter-Asset-Class)

Asset-Class	Variable	Abbreviation
Commodity	SPDR Gold Trust	GLD
Commodity	U.S. Oil Fund	USO
Currency	U.S. Dollar Index	USD
Fixed Income	U.S. IG Corporate Bond	LQD
Interest Rate	3M Treasury Yield	3M
Interest Rate	2Y Treasury Yield	2Y
Interest Rate	10Y Treasury Yield	10Y
Interest Rate	Fed Funds Effective Rate	FFEOR
Rate Spread	10Y-3M Spread	10Y-3M
Rate Spread	10Y-2Y Spread	10Y-2Y
Real Estate	U.S. Real Estate	IYR
Risk	CBOE Volatility Index	VIX
Sentiment	Bull-Bear Spread	BULL_BEAR_SPREAD

Table 6: Data Set 2 (Intra-Asset-Class)

Asset-Class	Variable
Commodity	Wheat Futures
Commodity	Corn Futures
Commodity	Copper Futures
Commodity	Silver Futures
Commodity	Gold Futures
Commodity	Platinum Futures
Commodity	Crude Oil Future
Commodity	Heating Oil Futures

The only data processing performed on the raw data is converting price data to return data and pre-processing any missing values. We use log returns for market variables, a standard practice in the financial domain. Log returns are used instead of regular differences because they result in more convenient downstream computations. Other data points are converted to regular differences because their values are much smaller and require higher precision. Market variables (that are transformed to log return, LR) for Data Set 1 is $\mathbf{LR}_1 := \{GLD, USO, USD, LQD, IYR, VIX\}$, while for Data Set 2 is $\mathbf{LR}_2 \equiv \mathcal{U}_2$, which are all the variables listed in Table 6. Since $u \in \mathcal{U}$ are tradable—i.e., can be interacted with via the market, they are market variables

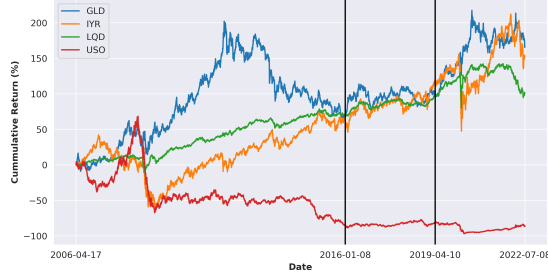


Figure 6: \mathcal{U} of Macro ETFs (Data Set 1)

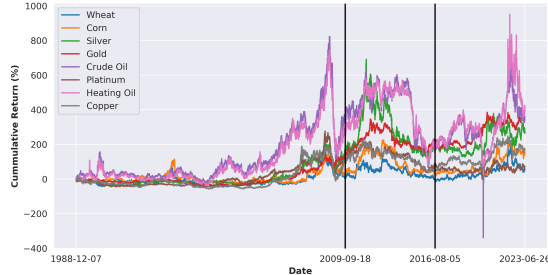


Figure 7: \mathcal{U} of Commodity Futures (Data Set 2)

by definition. Therefore, $\mathcal{U} \subseteq \mathbf{LR}$. In Data Set 1, \exists non market variables $\mathbf{LR}'_1 = \{3M, 2Y, 10Y, FFEOR, 10Y - 3M, 10Y - 2Y, BULLBEARSPREAD\}$. This distinction is useful for the data processing and the state representation method we present in Appendix Section 2. The pseudo-code for the data processing is provided in Algorithm 1.

2. State Representation

By the MDP framework, the decision-making $\forall t$ can be made only given \mathcal{S}_t . That is, all necessary information for optimizing π_t should be available in \mathcal{S}_t . Various methods exist to generate a state representation that captures historical data points. In preliminary tests, we examine an LSTM-based context vector for summarizing historical data points \mathcal{S}_t ; however, we find no meaningful improvement in control performance with a rise in computational run-time. We found a simple heuristic representation where T' is tuned in the training and validation set, which was computationally resource-efficient and worked consistently well. Hyperparameter T' corresponds to State Lag in Tables 9 and 10.

The search space for T' was $T'_{searchspace} := \{5, 10, \dots, 55, 60\}$ where, e.g., $T' := 5$ would mean that information on the last five data points are incorporated in \mathcal{S} . However, to avoid very large $|\mathcal{S}|$, we include the past 5 cumulative returns up to $t - 5$, but after that, every increase of 5 adds one additional element to \mathcal{S} . E.g., $T' := 20 \Rightarrow |\mathcal{S}_{T'}| = 5 + (1 \cdot 3) = 8$. This is better understood via the state representation generating pseudo-code in Algorithm 2.

3. Hyperparameters

Notably, for a fair comparison, we keep the hyperparameters overlapping across underlying algorithms and methods fixed to compare them. Concretely, \exists set of overlapping hyperparameters, $\mathcal{H} \forall$ (Data Set, Underlying RL Algorithm) pair, therefore in aggregate $|\mathcal{H}| = 6 \leftarrow 2 \cdot 3$ are used here. $\forall h \in \mathcal{H}$ is tuned by training on the train set and optimizing on the validation set. The optimized hyperparameters are available in Tables 7, 8, 9, and 10. One additional hyperparameter exists for the OPD method—distillation loss coefficient, which was tuned to 0.5. We use random grid search and Bayesian optimization for hyperparameter tuning—with implementation details in Appendix sections 3, 4, 5, and 6.

Table 7: Learned Gaussian Noise: Σ

Method	Data Set 1	Data Set 2
σ	1.628	2.170

Table 8: Tuned Inverse Smoothing Hyperparameter: S

Method	Data Set 1	Data Set 2
TRPO-TIS	8	1
PPO-TIS	3	7
A2C-TIS	8	1

Table 9: Tuned $h \in \mathcal{H}$ for Data Set 1

h	TRPO	PPO	A2C
Learning Rate	0.0001	0.0001	0.0001
State Lag	10	10	10
Steps per Update	292	292	292
Partition Factor for Batch Size	4	4	—
Epochs	—	8	—
Discount Factor	0.956	0.956	0.956
Bias-Variance Trade-off Factor	0.94	0.94	0.94
Clipping Parameter	—	0.6	—
Entropy Coefficient	—	0.03	0.03
Value Function Coefficient	—	4.6	4.6
Conjugate Gradient Max Steps	15	—	—
Hessian Dampening	0.1	—	—
Line Search Reduction Factor	0.8	—	—
Line Search Maximum Iteration	10	—	—
Critic Updates per Policy Update	10	—	—
Target KL Divergence	0.01	—	—
Sub-sampling Factor	1	—	—
Max Gradient Clipping	—	—	0.6
RMSProp Epsilon	—	—	0.0

4. Training Baselines

RP is a heuristic-based deterministic baseline and does not need training. On the contrary, TRPO, PPO, and A2C need training. The pseudo-code is presented in Algorithm 3. The subscript in $TrainModel()$ is the number of MDP steps the neural-network is trained on. $tune_sample_count := 150$ and $tune_step_size := 100,000$ for all methods, including

Algorithm 1: Data Process

Input: $data_{raw}$ **Output:** $data_{processed}$ $init\ data_{processed}$ $\mathbf{F} \leftarrow data_{raw}.get_feature_set()$ **for** $f \in \mathbf{F}$ **do****if** f **is** *MarketVariable* **then** $\forall data_{processed}[f].datapoint[i] \leftarrow \log(data_{raw}[f].datapoint[i]/data_{raw}[f].datapoint[i-1])$ **else if** $f.datapoints \neq nan$ **then** $\forall data_{processed}[f].datapoint[i] \leftarrow data_{raw}[f].datapoint[i] - data_{raw}[f].datapoint[i-1]$ **else** $\forall data_{processed}[f].datapoint[i] \leftarrow data_{raw}[f].datapoint[i] - data_{raw}[f].datapoint[most_recent_non_nan_i < i]$ **end if****end for** $data_{processed}[\mathbf{F}].datapoint[0].drop_timestep()$ **return** $data_{processed}$

Algorithm 2: State Representation

Input: $data_{processed}$, \mathbf{LR} , \mathbf{LR}' , T' **Output:** \mathcal{S}_t 1: *init vector* \mathcal{S}_t , $state_{LR}$, $state_{LR}'$ 2: $state_{LR}' \leftarrow data_{processed}[t-1][\mathbf{LR}']$

3:

4: **for** $feature \in \mathbf{LR}$ **do**5: *init vector* $temp$ 6: $lag_{size} \leftarrow 5 + (T' - 5)/5$

7:

8: **for** $i \in \{0, 1, \dots, lag_{size}\}$ **do**9: **if** $i < 6$ **then**10: $temp.append(sum(data_{processed}[t-1-i : t-1][feature]))$ 11: **else**12: $i \leftarrow (i - 5) * 5 + 5$ 13: $temp.append(sum(data_{processed}[t-1-i : t-1][feature]))$ 14: **end if**15: **end for**

16:

17: $state_{LR}.append(temp)$ 18: $state_{LR} \leftarrow Reshape(state_{LR}, (-1))$ 19: **end for**

20:

21: $\mathcal{S}_t \leftarrow Concat(state_{LR}', state_{LR})$ 22: **return** \mathcal{S}_t

IL and CL. All training for the models presented in this paper is done on machines up to a single RTX 3090, 16 CPU cores (32 threads), and 32 GB of RAM. This means that computationally weaker units have also been used to train numerous experiments in parallel.

5. Imitation Learning Training

The pseudo-code for IL methods is presented in Algorithm 4. The original work (Fang et al. 2021) can be reviewed for

a detailed implementation of OPD. The DPD framework is presented in the main body.

Notably, ϕ does not require the *state_lag* hyperparameter as historical values are useless for an oracle (future-seeing). Also, ϕ is trained for 5,000,000 steps to ensure a global optima. In DPD, lines 6 and 7 corresponding to finding a global optima, can be achieved via any method—including analytical. We identify that 5,000,000 steps are more than enough to find a global optima using RL. Since the global optima of

Algorithm 3: TRPO, PPO, A2C Training

Input: $data_{processed}$, $\mathcal{H}_{searchspace}$, $split_ratio$, $test_sample_count$, $tune_sample_count$, $tune_step_size$
Output: $\pi_{trained}$, \mathcal{H}^*

```

1:  $data_{train}, data_{validation}, data_{test} \leftarrow split\_ratio(data_{processed})$ 
2:
3:  $samples \leftarrow RandomGridSearch(\mathcal{H}_{searchspace}, data_{train}, data_{validation}, tune\_step\_size,$ 
    $tune\_sample\_count)$ 
4:  $\mathcal{H}^* \leftarrow arg\_max(samples.r \in \mathcal{R}_{validation})$ 
5:
6:  $data_{train} \leftarrow Concat(data_{train}, data_{validation})$ 
7:
8: for  $\{0, 1, \dots, test\_sample\_count - 1\}$  do
9:    $\pi_{trained} \leftarrow TrainModel_{1,000,000}(data_{train}, \mathcal{H}^*, AdamOptimizer)$ 
10:   $\pi_{trained}.append(\pi_{trained})$ 
11: end for
12: return  $\pi_{trained}, \mathcal{H}^*$ 

```

 Table 10: Tuned $h \in \mathcal{H}$ for Data Set 2

h	TRPO	PPO	A2C
Learning Rate	0.01	0.01	0.01
State Lag	45	45	45
Steps per Update	73	73	73
Partition Factor for Batch Size	2	2	—
Epochs	—	11	—
Discount Factor	0.908	0.908	0.908
Bias-Variance Trade-off Factor	0.94	0.94	0.94
Clipping Parameter	—	0.35	—
Entropy Coefficient	—	0.02	0.02
Value Function Coefficient	—	0.5	0.5
Conjugate Gradient Max Steps	15	—	—
Hessian Dampening	0.1	—	—
Line Search Reduction Factor	0.8	—	—
Line Search Maximum Iteration	10	—	—
Critic Updates per Policy Update	10	—	—
Target KL Divergence	0.01	—	—
Sub-sampling Factor	1	—	—
Max Gradient Clipping	—	—	0.6
RMSProp Epsilon	—	—	0.0

historical data is deterministic, we only need to train the ϕ once to extract the optimal trajectory.

6. Imitation Learning Ablation Training

DPD-LGN training is presented in Algorithm 5. The only added change is the label space for the student—the codomain of π^ϕ , which has now been perturbed via a Gaussian process. (Kandasamy et al. 2020)’s parallel Bayesian optimizer is used with a bandit optimizer and Euclidean distance.

7. Curriculum Learning and Ablation Training

All methods presented under CL apply some form of data augmentation only during training. Inference on the validation and test set are never augmented to preserve maximum likelihood properties in estimating out-sample p_{data} . Notably, during training, both the state space \mathcal{S} and label

space $r \in \mathcal{R}$ are smoothed. R and EMA are presented in Algorithm 6, while IS and TIS are presented in Algorithm 7 and 8. $S_{searchspace} := \{0, 1, \dots, 8\}$ for TIS, while $S_{searchspace} := \{\#\}$ for IS#, where $\# \in \mathbb{N}$ of choice. In our case, IS8 corresponds to $S_{searchspace} := \{8\}$.

8. Inference

The pseudo-code for inference is available in Algorithm 9. Results of PPO-based methods are presented in the main body, Figures 4 and 5. Results of TRPO and A2C-based methods are presented in Appendix Figures 8, 9, 10, and 11.

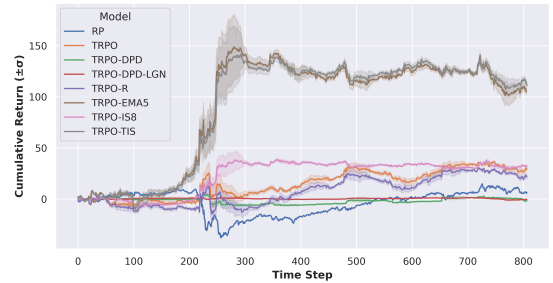


Figure 8: TRPO Test Set Inference (Data Set 1)

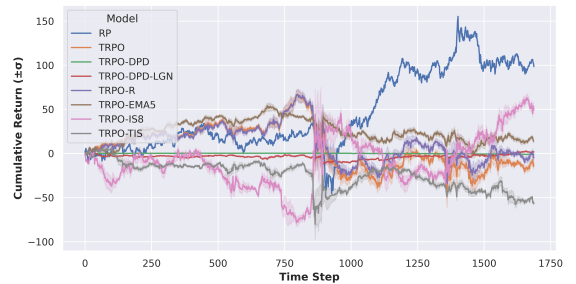


Figure 9: TRPO Test Set Inference (Data Set 2)

Algorithm 4: OPD, DPD Training

Input: $data_{processed}, \mathcal{H}_{searchspace}^{IL}, \mathcal{H}^*, split_ratio, test_sample_count, tune_sample_count, tune_step_size$ **Output:** $\pi_{trained}, \mathcal{H}^{\psi^*}$

```
1:  $data_{train}, data_{validation}, data_{test} \leftarrow split\_ratio(data_{processed})$ 
2:
3:  $samples^\phi \leftarrow RandomGridSearch^\phi(\mathcal{H}_{searchspace}^{IL}, \mathcal{H}^* \setminus \{state\_lag\}, data_{train}, data_{validation},$ 
    $tune\_step\_size, tune\_sample\_count)$ 
4:  $\mathcal{H}^{\phi^*} \leftarrow arg\_max(samples^\phi.r \in \mathcal{R}_{validation})$ 
5:
6:  $\pi^\phi \leftarrow TrainModel_{5,000,000}(data_{train}, data_{validation}, \mathcal{H}^{\phi^*}, AdamOptimizer)$ 
7:
8:  $samples^\psi \leftarrow RandomGridSearch^\psi(\pi^\phi, \mathcal{H}_{searchspace}^{IL}, \mathcal{H}^*, data_{train}, data_{validation},$ 
    $tune\_step\_size, tune\_sample\_count)$ 
9:  $\mathcal{H}^{\psi^*} \leftarrow arg\_max(samples^\psi.r \in \mathcal{R}_{validation})$ 
10:
11:  $data_{train} \leftarrow Concat(data_{train}, data_{validation})$ 
12:
13: for  $\{0, 1, \dots, test\_sample\_count - 1\}$  do
14:   if OPD then
15:      $\pi_{trained}^\psi \leftarrow ImitationTrainModel_{1,000,000}^{OPD}(\pi^\phi, data_{train}, \mathcal{H}^{\psi^*}, \mathcal{H}^*, AdamOptimizer)$ 
16:   else
17:      $\pi_{trained}^\psi \leftarrow ImitationTrainModel_{1,000,000}^{DPD}(\pi^\phi, data_{train}, \mathcal{H}^{\psi^*}, \mathcal{H}^*, AdamOptimizer)$ 
18:   end if
19:    $\pi_{trained}.append(\pi_{trained}^\psi)$ 
20: end for
21: return  $\pi_{trained}, \mathcal{H}^{\psi^*}, \pi^\phi$ 
```

Algorithm 5: DPD-LGN Training

Input: $data_{processed}, \mathcal{H}^{\psi^*}, \mathcal{H}^*, \pi^\phi, \sigma_{searchspace}, split_ratio, test_sample_count, tune_sample_count, tune_step_size$ **Output:** $\pi_{trained}$

```
1:  $data_{train}, data_{validation}, data_{test} \leftarrow split\_ratio(data_{processed})$ 
2:
3:  $\Sigma^* \leftarrow ParallelBayesianOptimizer(\sigma_{searchspace}, \mathcal{H}^{\psi^*}, \mathcal{H}^*, \pi^\phi, data_{train}, data_{validation}, tune\_step\_size,$ 
    $tune\_sample\_count)$ 
4:  $\pi^\phi \leftarrow GaussianPerturbation(\pi^\phi, \mu := 0, \Sigma := \Sigma^*)$ 
5:
6:  $data_{train} \leftarrow Concat(data_{train}, data_{validation})$ 
7:
8: for  $\{0, 1, \dots, test\_sample\_count - 1\}$  do
9:    $\pi_{trained}^\psi \leftarrow ImitationTrainModel_{1,000,000}(\pi^\phi, data_{train}, hyperparameters, AdamOptimizer)$ 
10:   $\pi_{trained}.append(\pi_{trained}^\psi)$ 
11: end for
12: return  $\pi_{trained}$ 
```

9. Statistical Significance

Tables 11, 12, and 13 show the one-sided difference T-statistic and corresponding P-values.

10. Noise Tolerance Mechanism under Constraints

We now discuss how our DPD framework, a simple yet pure form of IL, reduces the effects of $\Delta noise$ in the label space when the MDP environment is constrained. These constraints are innately required in financial control as capital is finite, and investment managers are given risk mandates. Our two representative constraints applied to Data Set

1 and Data Set 2, respectively, are available in Equation (4).

First, examine the state of the vanilla (single-learner)—i.e., the input space. $\forall t \exists \mathcal{S}_{T'} := \{\mathcal{SEC}_{t-1}^S, \dots, \mathcal{SEC}_{t-T'}^S\}$, where $T' \in \mathbb{N}$, $\mathcal{SEC}_t^S := \{\Delta signal_t^1 + \Delta noise_t^1, \dots, \Delta signal_t^m + \Delta noise_t^m\}$, $m := N$. Similarly, the space that affects the label space, that in turn affects π can be described as $\forall t \exists \mathcal{L}_T := \{\mathcal{SEC}_t^L, \dots, \mathcal{SEC}_{t+T}^L\}$, where $T \in \mathbb{N}$, $\mathcal{SEC}_t^L := \{\Delta signal_t^1 + \Delta noise_t^1, \dots, \Delta signal_t^p + \Delta noise_t^p\}$, $p \in \mathbb{N}$. $m := N$ does not necessarily have to equal p . $m = N = p$ is a unique case where $\mathcal{S} \equiv \mathcal{U}$, as in our Commodity

Table 11: Statistical Significance against TRPO in Test Set Cumulative Return ($\pm 1\sigma$)

Method	Data Set 1	T-stat 1	P-val 1 (%)	Data Set 2	T-stat 2	P-val 2 (%)
Heuristic						
RP	2.951	—	—	91.057	—	—
Baseline						
TRPO	29.440 \pm 51.712	—	—	-12.820 \pm 38.931	—	—
Imitation Learning*						
TRPO-DPD	-1.762 \pm 19.492	3.99	99.99	-0.9014 \pm 3.239	-2.16	1.79
TRPO-DPD-LGN [†]	-0.187 \pm 17.948	3.83	99.98	1.849 \pm 72.434	-1.26	10.55
Curriculum Learning*						
TRPO-R [‡]	21.949 \pm 61.999	0.66	74.33	-4.260 \pm 49.437	-0.96	16.93
TRPO-EMA5	104.599 \pm 44.225	-7.81	0.00	13.941 \pm 67.672	-2.42	0.88
TRPO-IS8	31.806 \pm 29.014	-0.28	38.93	49.471 \pm 112.507	-3.70	0.02
TRPO-TIS [†]	111.169 \pm 44.182	-8.50	0.00	-56.721 \pm 130.088	2.29	98.70

*ours, [†]ablation study, [‡]naïve approachTable 12: Statistical Significance against PPO in Test Set Cumulative Return ($\pm 1\sigma$)

Method	Data Set 1	T-stat 1	P-val 1 (%)	Data Set 2	T-stat 2	P-val 2 (%)
Heuristic						
RP	2.951	—	—	91.057	—	—
Baselines						
PPO	29.440 \pm 51.712	—	—	4.202 \pm 64.185	—	—
PPO-OPD	23.009 \pm 48.459	0.64	73.87	-44.461 \pm 177.441	1.82	96.35
Imitation Learning*						
PPO-DPD	3.543 \pm 29.152	3.08	99.86	-24.805 \pm 79.796	2.00	97.60
PPO-DPD-LGN [†]	-3.059 \pm 35.961	3.65	99.98	-4.687 \pm 100.238	0.53	70.06
Curriculum Learning*						
PPO-R [‡]	17.028 \pm 50.973	1.20	88.52	-13.728 \pm 69.622	1.33	90.81
PPO-EMA5	81.817 \pm 33.423	-6.01	0.00	35.215 \pm 55.376	0.26	0.56
PPO-IS8	81.873 \pm 39.850	-5.68	0.00	39.389 \pm 134.199	-1.673	4.88
PPO-TIS [†]	28.032 \pm 53.716	0.13	55.30	24.380 \pm 120.121	-1.05	14.91

*ours, [†]ablation study, [‡]naïve approach

Algorithm 6: R, EMA Training

Input: $data_{processed}$, \mathcal{H}^* , $split_ratio$, $test_sample_count$, $tune_sample_count$, $tune_step_size$, $rounding_parameter$ or w_l

Output: $\pi_{trained}$

```
1:  $data_{train}, data_{validation}, data_{test} \leftarrow split\_ratio(data_{processed})$ 
2:  $data_{train} \leftarrow Concat(data_{train}, data_{validation})$ 
3:  $data_{train} \leftarrow Smoothing(data_{train}, rounding\_parameter \text{ or } w_l)$ 
4:
5: for  $\{0, 1, \dots, test\_sample\_count - 1\}$  do
6:    $\pi_{trained} \leftarrow TrainModel_{1,000,000}(data_{train}, \mathcal{H}^*, AdamOptimizer)$ 
7:    $\pi_{trained}.append(\pi_{trained})$ 
8: end for
9: return  $\pi_{trained}$ 
```

Algorithm 7: IS, TIS Training

Input: $data_{processed}$, \mathcal{H}^* , $split_ratio$, $test_sample_count$, $tune_sample_count$, $tune_step_size$, $S_{searchspace}$

Output: $\pi_{trained}$

```
1:  $data_{train}, data_{validation}, data_{test} \leftarrow split\_ratio(data_{processed})$ 
2: if  $|S_{searchspace}| \equiv 1$  then
3:    $S^* \leftarrow S \in S_{searchspace}$ 
4:    $data_{train} \leftarrow IS(Concat(data_{train}, data_{validation}), S^*)$ 
5: else
6:   for  $S \in S_{searchspace}$  do
7:      $data_{train} \leftarrow IS(data_{train}, S)$ 
8:      $\pi \leftarrow TrainModel_{1,000,000}(data_{train}, \mathcal{H}^*)$ 
9:      $samples.append(Inference(data_{validation}, \pi))$ 
10:  end for
11:   $S^* \leftarrow arg\_max(samples.r \in \mathcal{R}_{validation})$ 
12:   $data_{train} \leftarrow IS(Concat(data_{train}, data_{validation}), S^*)$ 
13: end if
14:
15: for  $\{0, 1, \dots, test\_sample\_count - 1\}$  do
16:    $\pi_{trained} \leftarrow TrainModel_{1,000,000}(data_{train}, \mathcal{H}^*, AdamOptimizer)$ 
17:    $\pi_{trained}.append(\pi_{trained})$ 
18: end for
19: return  $\pi_{trained}$ 
```

Algorithm 8: IS(\cdot, \cdot)

Input: $data_{train}, S$

Output: $data_{train}$

```
1:  $partition\_size \leftarrow floor(|data_{train}|/S)$ 
2:  $i \leftarrow 0$ 
3: for  $j \in \{S - 1, S - 2, \dots, 0\}$  do
4:    $data_{train}[i(partition\_size):(i + 1)(partition\_size)] \leftarrow EMA(data_{train}[i(partition\_size):(i + 1)(partition\_size)]),$ 
      $w_l := j)$ 
5:    $i ++$ 
6: end for
7: return  $data_{train}$ 
```

Futures MDP environment corresponding to Data Set 2.

The noise tolerance mechanism of $\pi^\psi : \mathcal{S}_{T'} \times \mathcal{A}^\phi \mapsto a$ process is best introduced via an example. Suppose $\mathcal{U} := \{sec_1, \dots, sec_4\}$, which π expects will change by 1.23, 1.79, 3.01, and -4.02 percent on average, respectively. Now suppose a π is asked to give an a vector of size four of discrete

values $\in [-1, 0, 1]$ representing whether to take a short, none, or long position $\forall sec$. As the reward (label) is calculated via portfolio return, the a vector is again transformed, $w(a)$, to conform to the constraints. Suppose the constraint is that the position magnitude must always add up to 1—the same constraint given to the first MDP environment, Data

Algorithm 9: Inference

Input: $\pi_{trained}, MDP$
Output:

```

1: for  $\pi \in \pi_{trained}$  do
2:    $\mathcal{S} \leftarrow MDP.reset()$ 
3:
4:   while true do
5:      $action, _states \leftarrow \pi(\mathcal{S})$ 
6:      $\mathcal{S}, reward, done, _info \leftarrow MDP.step(action)$ 
7:     if done then
8:       break
9:     end if
10:  end while
11:
12: end for
13: return

```

 Table 13: Statistical Significance against A2C in Test Set Cumulative Return ($\pm 1\sigma$)

Method	Data Set 1	T-stat 1	P-val 1 (%)	Data Set 2	T-stat 2	P-val 2 (%)
Heuristic						
RP	2.951	—	—	91.057	—	—
Baseline						
A2C	9.374 \pm 33.604	—	—	9.567 \pm 66.664	—	—
Imitation Learning*						
A2C-DPD	1.205 \pm 40.249	1.10	86.33	0.099 \pm 4.680	1.00	83.93
A2C-DPD-LGN [†]	9.613 \pm 41.123	-0.03	48.73	1.043 \pm 15.055	0.88	80.91
Curriculum Learning*						
A2C-R [‡]	7.493 \pm 32.060	0.29	61.24	5.893 \pm 72.870	0.26	60.35
A2C-EMA5	40.550 \pm 24.504	-5.30	0.00	104.17 \pm 75.074	-6.66	0.00
A2C-IS8	46.018 \pm 28.972	-5.85	0.00	41.937 \pm 106.385	-1.82	3.60
A2C-TIS [†]	46.414 \pm 28.788	-5.92	0.00	4.651 \pm 130.721	0.24	59.34

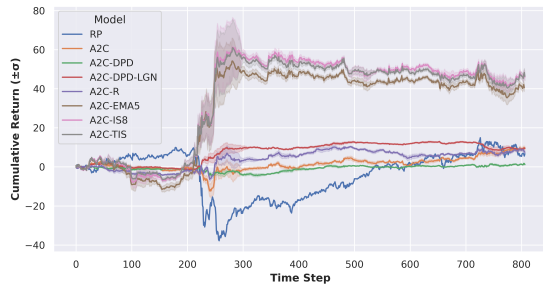
 *ours, [†]ablation study, [‡]naïve approach


Figure 10: A2C Test Set Inference (Data Set 1)

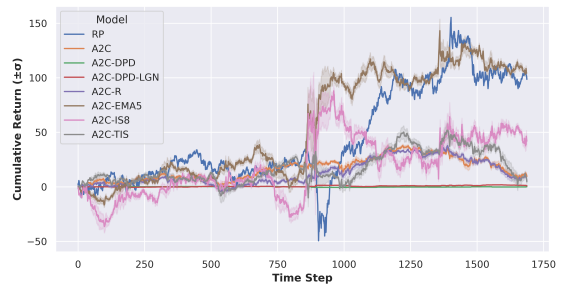


Figure 11: A2C Test Set Inference (Data Set 2)

Set 1. In our case, we use a simple normalization method to respect the hard constraints. However, another common approach would be to use softmax. Nevertheless, since both approaches are deterministic, the logic holds. In this environment, the deterministic $\mathcal{A}^* = [0, 0, 0, -1]$ as allocating

the entire portfolio to a short position in sec_4 yields the maximum expected return of 4.02 percent.

Now, given that π^ψ learns to assign -1 to sec_4 and zero to the remaining sec , via imitating the ϕ , \exists a degree of noise-tolerance, $\mathcal{DN}\mathcal{T}$. $\mathcal{DN}\mathcal{T}$ is

$$\underset{sec \in \mathcal{U}}{\text{rank}}^{i:=0}_{\text{descending}} |E[\Delta sec_t]| - \underset{sec \in \mathcal{U}}{\text{rank}}^{i:=1}_{\text{descending}} |E[\Delta sec_t]| \quad (6)$$

, which evaluates to $4.02 - 3.01 = 1.01$ in our example theoretical case. Translating to an additional $\partial \Delta noise < 1.01$ tolerable $\forall \Delta sec$ without affecting the training of the ψ learner. The formalization of the idea is described below.

Definition 1 *Degree of Noise-tolerance, $\mathcal{DNT} \in \mathbb{R} \geq 0$ is the maximum additional noise tolerable for each element in an expected movement vector s.t. the constraint-respecting weight vector remains unchanged. Formally, it can be described as the following. Given a state-action mapping*

$$\pi_t : \mathcal{S}_{T'} \mapsto a_t \quad (7)$$

$$\text{s.t. } \arg \min_{\pi} -\mathbb{E}(r(\mathcal{W}) | \mathcal{S}, \pi_{\theta}), \quad (8)$$

and a consequent deterministic transformation of a to w , described by CN , where

$$CN : a_t \mapsto w_t, \quad (9)$$

s.t. w respects the constraints of the portfolio environment, \exists by the temporal nature of π_t , abstracted implicit reasoning of

$$\mathbb{E}[\Delta sec_t | \mathcal{S}_{T'}], \forall sec_t \in \mathcal{U}, \quad (10)$$

within the neural-network. Here, \mathcal{DNT} is defined as, $\forall sec \in \mathcal{U}$, the following inequality holds:

$$\partial |\mathbb{E}[\Delta sec_t | \mathcal{S}_{T'}]| < \mathcal{DNT}, \text{ s.t. } \Delta a_t = 0 \quad (11)$$

where $\partial |\mathbb{E}[\cdot]|$ expresses any additional noise, and $\Delta a = 0$ expresses no change in action vector, a . Naturally, $\Delta w = 0$.

This definition is specific for the environment constraints given in this paper. \mathcal{DNT} would be defined differently for different environment constraints. Unlike the vanilla learner, where the \mathcal{R} is derived from \mathcal{L}_T , the student learner's \mathcal{R} is derived from the teacher's optimal \mathcal{A}^* vector, which has \mathcal{DNT} properties. This does not entirely remove the noise's impact on learning, but does reduce its effect—i.e., the learning system is tolerant to some level of noise. With the example in-hand, a one percent increase of noise in the expected movement of any single sec would change the r_t^{vanilla} , but no change in r_t^{ψ} will be observed. In turn, it is synthetically achieving significantly lower $\Delta noise$ in the label space. However, as seen in the main text, this also results in significant removal $\Delta signal$, which is detrimental to learning the parameters.